

## Article

# Humic Acid-Coated Fe<sub>3</sub>O<sub>4</sub> Nanoparticles Confer Resistance to Acremonium Wilt Disease and Improve Physiological and Morphological Attributes of Grain Sorghum

Sherif Mohamed El-Ganainy <sup>1,2,\*</sup> , Amal M. El-Bakery <sup>3</sup>, Heba M. Hafez <sup>4</sup>, Ahmed Mahmoud Ismail <sup>2,\*</sup>, Ali Zein El-Abdeen <sup>3</sup>, Abed Abd Elgalel Ata <sup>3</sup>, Omar A. Y. Abd Elraheem <sup>4</sup>, Yousef M. Y. El Kady <sup>4</sup> , Ahlam F. Hamouda <sup>5</sup>, Hossam S. El-Beltagi <sup>6,7</sup> , Wael F. Shehata <sup>6</sup>, Tarek A. Shalaby <sup>1</sup> , Ahmed Osman Abbas <sup>8</sup>, Mustafa Ibrahim Almaghsala <sup>1</sup>, Muhammad N. Sattar <sup>9</sup> and Zafar Iqbal <sup>9</sup>

- <sup>1</sup> Department of Arid Land Agriculture, College of Agriculture & Food Sciences, King Faisal University, P.O. Box 420, Al-Ahsa 31982, Saudi Arabia; tshalaby@kfu.edu.sa (T.A.S.); malmghaslah@kfu.edu.sa (M.I.A.)
  - <sup>2</sup> Vegetable Diseases Research Department, Plant Pathology Research Institute, Agricultural Research Center (ARC), Giza 12619, Egypt
  - <sup>3</sup> Maize and Sugar Crops Diseases Research Department, Plant Pathology Research Institute, Agricultural Research Center (ARC), Giza 12619, Egypt; elbakry\_aml@yahoo.com (A.M.E.-B.); ali\_zein\_55@yahoo.com (A.Z.E.-A.); esraaabed1012004@gmail.com (A.A.E.A.)
  - <sup>4</sup> Department, of Sorghum Research, Field Crops Research Institute, Agricultural Research Center (ARC), Giza 12619, Egypt; hobahafez67@yahoo.com (H.M.H.); omar5556666omar@gamil.com (O.A.Y.A.E.); youssefelkady82@gmail.com (Y.M.Y.E.K.)
  - <sup>5</sup> Department of Forensic Medicine and Toxicology, Teaching Hospital, Faculty of Veterinary Medicine, Benha University, Benha 13736, Egypt; ahlamhamouda10@gmail.com
  - <sup>6</sup> Department of Agricultural Biotechnology, College of Agricultural and Food Science, King Faisal University, P.O. Box 400, Al-Ahsa 31982, Saudi Arabia; helbeltagi@kfu.edu.sa (H.S.E.-B.); wshehata@kfu.edu.sa (W.F.S.)
  - <sup>7</sup> Biochemistry Department, Faculty of Agriculture, Cairo University, Gamma St, Giza 12613, Egypt
  - <sup>8</sup> Department of Animal and Fish Production, College of Agricultural and Food Sciences, King Faisal University, P.O. Box 420, Al-Ahsa 31982, Saudi Arabia; aabbas@kfu.edu.sa
  - <sup>9</sup> Central laboratories, King Faisal University, P.O. Box 420, Al-Ahsa 31982, Saudi Arabia; mnsattar@kfu.edu.sa (M.N.S.); zafar@kfu.edu.sa (Z.I.)
- \* Correspondence: salganainy@kfu.edu.sa (S.M.E.-G.); ma.ah.ismail@gmail.com (A.M.I.)



**Citation:** El-Ganainy, S.M.; El-Bakery, A.M.; Hafez, H.M.; Ismail, A.M.; El-Abdeen, A.Z.; Ata, A.A.E.; Elraheem, O.A.Y.A.; El Kady, Y.M.Y.; Hamouda, A.F.; El-Beltagi, H.S.; et al. Humic Acid-Coated Fe<sub>3</sub>O<sub>4</sub> Nanoparticles Confer Resistance to Acremonium Wilt Disease and Improve Physiological and Morphological Attributes of Grain Sorghum. *Polymers* **2022**, *14*, 3099. <https://doi.org/10.3390/polym14153099>

Academic Editor: Dimitrios Bikiaris

Received: 25 June 2022

Accepted: 26 July 2022

Published: 30 July 2022

**Publisher's Note:** MDPI stays neutral with regard to jurisdictional claims in published maps and institutional affiliations.



**Copyright:** © 2022 by the authors. Licensee MDPI, Basel, Switzerland. This article is an open access article distributed under the terms and conditions of the Creative Commons Attribution (CC BY) license (<https://creativecommons.org/licenses/by/4.0/>).

**Abstract:** Acremonium wilt disease affects grain quality and reduces sorghum yield around the globe. The present study aimed to assess the efficacy of humic acid (HA)-coated Fe<sub>3</sub>O<sub>4</sub> (Fe<sub>3</sub>O<sub>4</sub>/HA) nanoparticles (NPs) in controlling acremonium wilt disease and improving sorghum growth and yields. During the season 2019, twenty-one sorghum genotypes were screened to assess their response to *Acremonium strictum* via artificial infection under field conditions and each genotype was assigned to one of six groups, ranging from highly susceptible to highly resistant. Subsequently, over the two successive seasons 2020 and 2021, three different concentrations of 10, 40 and 80 mg L<sup>-1</sup> of Fe<sub>3</sub>O<sub>4</sub>/HA NPs were tested against *A. strictum*. The concentrations of 40 and 80 mg L<sup>-1</sup> were found to be highly effective in controlling acremonium wilt disease on different sorghum genotypes: LG1 (highly susceptible), Giza-3 (susceptible), and Local 119 (resistant) genotypes. After harvest, the physiological (growth and yield) and biochemical (peroxidase, catalase, and gibberellic acid) attributes of sorghum plants were determined, and the results demonstrated that concentrations of 40 and 80 mg L<sup>-1</sup> increased peroxidase and catalase activities in healthy (uninoculated) sorghum genotypes compared to inoculated sorghum genotypes. Additionally, the toxicity of Fe<sub>3</sub>O<sub>4</sub>/HA NPs on male albino rats was investigated via hematological (CBC), chemical (ALT and AST) and histopathological analyses. The concentration 80 mg L<sup>-1</sup> of Fe<sub>3</sub>O<sub>4</sub>/HA NPs caused a marked increase in ALT and creatinine level after 51 days of feeding. Severe pathological alterations were also observed in liver and kidney tissues of rats administered with grain sorghums treated with 80 mg L<sup>-1</sup>. In comparison with the untreated control plants, a concentration of 40 mg L<sup>-1</sup> significantly increased the growth, yield and gibberellic acid levels ( $p \leq 0.05$ ) and was found to be safe in male albino rats. Conclusively, a concentration of 40 mg L<sup>-1</sup> of Fe<sub>3</sub>O<sub>4</sub>/HA NPs showed promising results in curtailing *A. strictum* infections in

sorghum, indicating its great potential to substitute harmful fertilizers and fungicides as a smart agriculture strategy.

**Keywords:** *Acremonium strictum*; acremonium wilt; humic acid; iron oxide nanoparticles; grain sorghum; toxicity

## 1. Introduction

Sorghum (*Sorghum bicolor* L. Moench) is one of the most important cereal crops in Egypt and worldwide. It ranks fifth in production after wheat, rice, maize and barley, with an annual global production of 58.71 million tons from a cultivation area of 40.21 million hectares [1]. Acremonium wilt of Sorghum caused by *Acremonium strictum* Gams (also referred to as *Cephalosporium acremonium* Cord) is a leading cause of yield losses (15–60%) to susceptible sorghum cultivars [2,3]. *A. strictum* directly affects sorghum production by poor grain filling or indirectly through lodging or stalk breakage [4–6]. The disease is predominating in upper Egypt [7], where the environmental conditions are favorable for sorghum production. Acremonium wilt is not considered as a stalk rot disease because *A. strictum* behaves like a true vascular soil-borne fungus, while stalk-rotting fungi are frequently found in wilted plants, therefore *A. strictum* acts as a predisposing agent.

Smart agriculture is a contemporary approach to achieve sustainability, both short- and long-term, in the countenance of climate change [8,9]. Therefore, the implementation of nanotechnology research in plant protection and production in the agriculture sector is a critical key factor for sustainable developments [10]. Metal-based nanomaterials (NPs) have a much greater surface area-to-volume ratio and unique antimicrobial effects compared to their normal forms. Different NPs have successfully been used to control different fungal, bacterial and viral plant pathogens [10–18]. Iron-oxide-based nanomaterials have become of great interest to scientists and researchers due to their favorable magnetic and electrical properties. They have many interesting applications in industry [19–23], medicine and biology [24,25]. Iron oxide nanomaterials were mainly divided into three types, i.e.,  $\alpha$ -Fe<sub>2</sub>O<sub>3</sub>,  $\gamma$ -Fe<sub>2</sub>O<sub>3</sub> and Fe<sub>3</sub>O<sub>4</sub>. Among all, maghemite ( $\gamma$ -Fe<sub>2</sub>O<sub>3</sub>) and magnetite (Fe<sub>3</sub>O<sub>4</sub>) are mostly studied [26,27] and frequently used due to their strong magnetic targeting and structural features [28]. However, Fe<sub>3</sub>O<sub>4</sub> NPs, stand-alone, have a tendency for agglomeration, due to strong magnetic attraction among particles through van der Waals forces [29]. Therefore, the coating of NPs is an excellent technique for enhancing their properties through electrostatic stabilization among particles and can decrease their agglomeration [30]. The surface coating of NPs is accomplished with a variety of materials, including bioactive compounds, organic and inorganic compounds, as well as natural and synthetic polymers [31]. HA is a natural organic matter containing alkyl and aromatic units attached with carboxylic acid, phenolic hydroxyl and quinone functional groups that can form complexes with iron and iron oxide [32]. HA is referred to as agricultural black gold, which is a prolific constituent of humic substances and is distributed in the environment. HA contains a high concentration of trace minerals and aids plant growth and is responsible for the structure and physio-chemical properties of soil. Humic substances in humin can be fractionated into fulvic acids, brown HA and grey HA based on their solubility at different pH levels. HA has a similar characteristic to Fe<sub>3</sub>O<sub>4</sub> NPs, including improved dispersion stability for NPs [33] and electrostatic stabilization over a wide range of pH [34]. The synthesis of iron oxide is the most important parameter in producing crystalline polymorphs with desirable and distinctive properties that make them suitable for technological applications. The synthesis of iron oxide NPs can be achieved physically [35], chemically [36] and biologically [37]. Physical methods are easy to perform, but controlling the particle size is difficult. While in wet chemical preparation, the particle size can be somewhat controlled by adjusting the conditions. Therefore, chemical-based synthesis methods are mostly adopted due to their appropriateness, low production cost and high yield [38].

The present study aimed to: (1) prepare HA-coated Fe<sub>3</sub>O<sub>4</sub> (Fe<sub>3</sub>O<sub>4</sub>/HA) NPs using a chemical co-precipitation method; (2) investigate the potential of Fe<sub>3</sub>O<sub>4</sub>/HA NPs in controlling the acremonium wilt disease of sorghum; (3) study its effect on growth and yield of Sorghum plants; and (4) investigate its potential toxicity on rats using chemical and histopathological investigations.

## 2. Materials and Methods

### 2.1. Preparations and Characterization of Coated Fe<sub>3</sub>O<sub>4</sub>/HA

HA coated Fe<sub>3</sub>O<sub>4</sub> NPs (Fe<sub>3</sub>O<sub>4</sub>/HA) was prepared in the Department of Corn Diseases and Sugar Crops, Agricultural Research Center (ARC), Egypt, through a chemical co-precipitation method [39]. The size and morphology of NPs were determined by Transmission electron microscopy (TEM, JEOL JEM 1400) at National Research Center (NRC), Cairo, Egypt. Imaging of surface morphology and structure was conducted using Scanning Electron Microscopy (SEM, Quanta FEG250). The presence of synthesized Fe<sub>3</sub>O<sub>4</sub>/HA NPs was confirmed with Energy Dispersive X-ray Spectrometer (EDX) [40,41] at NRC, Cairo, Egypt. Size distribution, zeta potential and poly disparity index (Pdi) of NPs in suspension were determined using DLS by Zeta sizer (Nano ZS, Malvern, UK) at Regional Center for Food and Feed. ARC, Egypt.

### 2.2. Source and Inoculum Preparation of *A. strictum*

*A. strictum* used in this study was previously isolated from sorghum plants showing acremonium wilt symptoms. The identity of *A. strictum* was confirmed based on morphological characteristics. The inoculum was prepared by culturing *A. strictum* on PDA medium for 6 days at 30 °C.

### 2.3. Effect of Fe<sub>3</sub>O<sub>4</sub>/HA Nanoparticles on the Mycelial Growth of *A. strictum*

Effect of Fe<sub>3</sub>O<sub>4</sub>/HA NPs on the mycelial growth of *A. strictum* was determined on the PDA medium supplemented with yeast extract using the Poison media technique [42]. The PDA medium supplemented with different concentrations (10, 40 and 80 mg L<sup>-1</sup>) of Fe<sub>3</sub>O<sub>4</sub>/HA NPs was poured into Petri dishes. After solidification, the plates were inoculated at the center with fresh mycelial agar plugs of *A. strictum* and incubated at 28 ± 2 °C for 6 days. PDA plates without supplementing Fe<sub>3</sub>O<sub>4</sub>/HA NPs inoculated with mycelial plugs of *A. strictum* were run as controls. The diameter of mycelial growth was measured in millimeters (mm) and inhibition ratio was calculated.

### 2.4. Reaction of Twenty-One Genotypes of Grain Sorghum to *A. strictum* under Field Conditions

Twenty-one genotypes of grain sorghums were screened for their reaction to *A. strictum* under field conditions during the growing season of 2019. The trials were carried out at Agricultural Research Center (ARC) Farm, Giza, Egypt. The experimental plot was comprised of two rows of 4 m each, 60 cm apart and 20 cm between hills. After three weeks of sowing, sorghum plants were thinned to two plants per hill. Fourteen days post-flowering, artificial inoculation was performed, approximately 10 cm above the ground, by piercing a sterile needle followed by inserting a toothpick containing *A. strictum* mycelia into plant stalk between the leaf sheath and the stalk [43]. Four weeks later, the stalks were longitudinally sectioned, and the disease rating was determined using the scale (Table 1). The infection levels, ranging from highly resistant to highly susceptible, were inferred according to the set criterion (Table 2) [44]. The experimental block design was completely randomized with three replicates for each genotype.

### 2.5. Effect of Fe<sub>3</sub>O<sub>4</sub>/HA Nanoparticles on *A. strictum* under Field Conditions

Fe<sub>3</sub>O<sub>4</sub>/HA NPs were evaluated for controlling *A. strictum* under field conditions during the seasons 2020 and 2021. Out of 21 genotypes, five sorghum genotypes, widely cultivated in Egypt, were selected after screening for their reaction to acremonium wilt disease in the first growing season (2019). A comparable experimental layout to the

evaluation of genotypes was used. Grain sorghums were soaked in different concentrations (10, 40 and 80 mg L<sup>-1</sup>) of Fe<sub>3</sub>O<sub>4</sub>/HA NPs for 24 h prior to sowing. Additionally, the foliar spray of Fe<sub>3</sub>O<sub>4</sub>/HA NPs was performed twice on the plants with the respective NP concentrations; the first spray was performed one week before inoculation and the second spray was performed one week after the inoculation. The control plants were sprayed with sterile water. Four weeks after inoculation, disease severity was determined using the rating scale (Table 1). The experimental design block was completely randomized using strip split plot arrangement with three replicates. Treatments with Fe<sub>3</sub>O<sub>4</sub>/HA NPs (10, 40 and 80 mg L<sup>-1</sup>) and the control were horizontally allocated. While the genotypes Giza 113, LG 1, LG 3, Giza 3 and local 119 were vertically arranged in sub-plots. These five selected genotypes represent four categories as follows: LG 1 was highly susceptible; LG 3 was moderately susceptible; Giza 113 and Giza 3 were sorted as susceptible, while Local 119 was considered as resistant.

**Table 1.** Disease rating scale adopted according to IDIN-instruction manual.

Numerical Grade	Degree of Infection
0.1	Minimal reaction, indistinguishable from that to a sterile toothpick.
0.2	Discoloration centered around the wound, progressing in the superficial parts of the stalk, but not reaching either node.
0.5	Extensive discoloration progressing in the central part of the stalk.
0.8	Discoloration reaching one or both nodes superficially or forming a cylinder.
1.0	Most or all of one internode discolored with no penetration of nodal areas.
1.1	Slight penetration of one or both nodes.
1.2	Nearly complete penetration of one or both nodes,
1.5	Penetration of one node and slight invasion of next internode.
2.0	More than one internode but not more than two affected; infection must have spread through at least one internode.
2.5	Penetration of two nodes and slight invasion of distal internode.
3.0	Infection passed through two or more internodes.
4.0	Extensive invasion of plant but not killed.
5.0	Death of plant due to stalk-rot.

**Table 2.** Category of *A. striticum* infestation based on numerical categorization and level of infection.

No.	Category Numerical	Level of Infection
1	0.0–0.5	Highly resistant
2	0.6–1.0	Resistant
3	1.1–1.5	Moderately resistant
4	1.6–3.0	Moderately susceptible
5	3.1–4.0	Susceptible
6	4.1–5.0	Highly Susceptible

## 2.6. Gibberellic Acid Assay

The effect of Fe<sub>3</sub>O<sub>4</sub>/HA NPs on gibberellic acid levels in the five genotypes was determined, as previously described [45]. Samples were collected after 75 days of sowing and gibberellic acid was quantified using gas chromatography–mass spectrometry (GC-MS; Agilent 7000 Triple Quad) at the Regional Center for Food and Feed, ARC, Giza, Egypt.

### 2.7. Assessment of Growth and Yield Parameters

Yield parameters including a weight of 1000 grains, grain yield per plant and plant heights were determined at harvest time for all plants in each plot.

### 2.8. Enzyme Assays

Enzymatic activities of peroxidase and catalase were determined in leaves of sorghum plants after 75 days of sowing. Samples were collected and extracted with Tris-HCl buffer and the extracts were centrifuged at 10,000 rpm for 15 min at 4 °C. The resulting supernatants were separated as enzyme extracts. The peroxidase activity was determined [46] and expressed as  $\Delta A 422 \text{ nm min}^{-1} \text{ g}^{-1} \text{ FW}$ . The catalase activity was determined [47] and expressed as  $\Delta A 240 \text{ nm min}^{-1} \text{ g}^{-1} \text{ FW}$ .

### 2.9. Potential Toxicity of Fe<sub>3</sub>O<sub>4</sub>/HA NPs on Rats

Twelve male albino rats (average weight 120–150 gm) were used to assess the potential toxicity of Fe<sub>3</sub>O<sub>4</sub>/HA NPs. Rats obtained from Lab Animal House, Faculty of Veterinary Medicine, Benha University, Egypt. They were housed in well-ventilated stainless-steel wire cages under laboratory conditions at temperature of 18–24 °C and 12 h light and darkness. The experimental protocol was developed in accordance to ethical guidelines (BUFVTM 07-04-22). Rats were acclimatized for 5 days before the treatments. Rats were randomly divided into four groups; three groups (3 rats each) were caged individually and were administered grain sorghums treated with different concentrations (10, 40 and 80 mg L<sup>-1</sup>) of Fe<sub>3</sub>O<sub>4</sub>/HA NPs. The fourth group rats were fed on untreated grain sorghums and served as the control group.

After 21, 36 and 51 days of feeding, blood samples of rats were collected and subjected to CBC tests; including RBCs count [48], Hb and white blood cells (WBCs) [49].

Blood serum was used to assess the activity of serum AST and ALT as a marker of liver function [50] and creatinine level as a marker of kidney function [51].

### 2.10. Histopathological Examination

After 51 days of feeding on Fe<sub>3</sub>O<sub>4</sub>/HA NPs, autopsy samples were taken from the liver and kidneys of rats in different groups and fixed in 10% formalin saline for 24 h. The samples were thoroughly washed with water before being dehydrated with serial alcohol (methyl, ethyl and absolute ethyl) dilutions. Specimens were cleared in xylene and embedded in paraffin for 24 h at 56 °C in a hot air oven. Paraffin bees wax tissue blocks were prepared for sectioning at 4 microns thickness (Rotary microtome, Leitz, Germany). Tissue sections were obtained on glass slides, deparaffinized and stained with hematoxylin & eosin (H&E) staining and finally examined under a light electric microscope [52].

### 2.11. Data Analysis

Data were subjected for analysis of variance using software DSAASTAT Version 1.1 [53]. Differences between the means were inferred by Fisher's protected least significant difference (LSD) at a level of 5% significance.

## 3. Results

### 3.1. Morphology and Size Distribution of Fe<sub>3</sub>O<sub>4</sub>/HA NPs

The TEM and SEM images confirmed that the Fe<sub>3</sub>O<sub>4</sub>/HA NPs were quasi-spherical in shape and had nearly uniform distribution, with particle sizes ranging from 60 to 72 nm (Figure 1A,C). The dynamic light scattering system (DLS) results revealed that the Fe<sub>3</sub>O<sub>4</sub>/HA NPs were heterogeneously distributed, with an average of approximately 174 nm representing 96% of the colloidal solution and a poly disparity index (Pdi) of 0.379 (Figure 1B). Zeta potential of Fe<sub>3</sub>O<sub>4</sub>/HA NPs exhibited a negative charge at −19.0 mv. The peaks of EDX results revealed the presence of iron, oxygen, carbon and other associated elements in the incorporated table (Figure 1E), therefore, confirming the synthesis of Fe<sub>3</sub>O<sub>4</sub>/HA NPs.

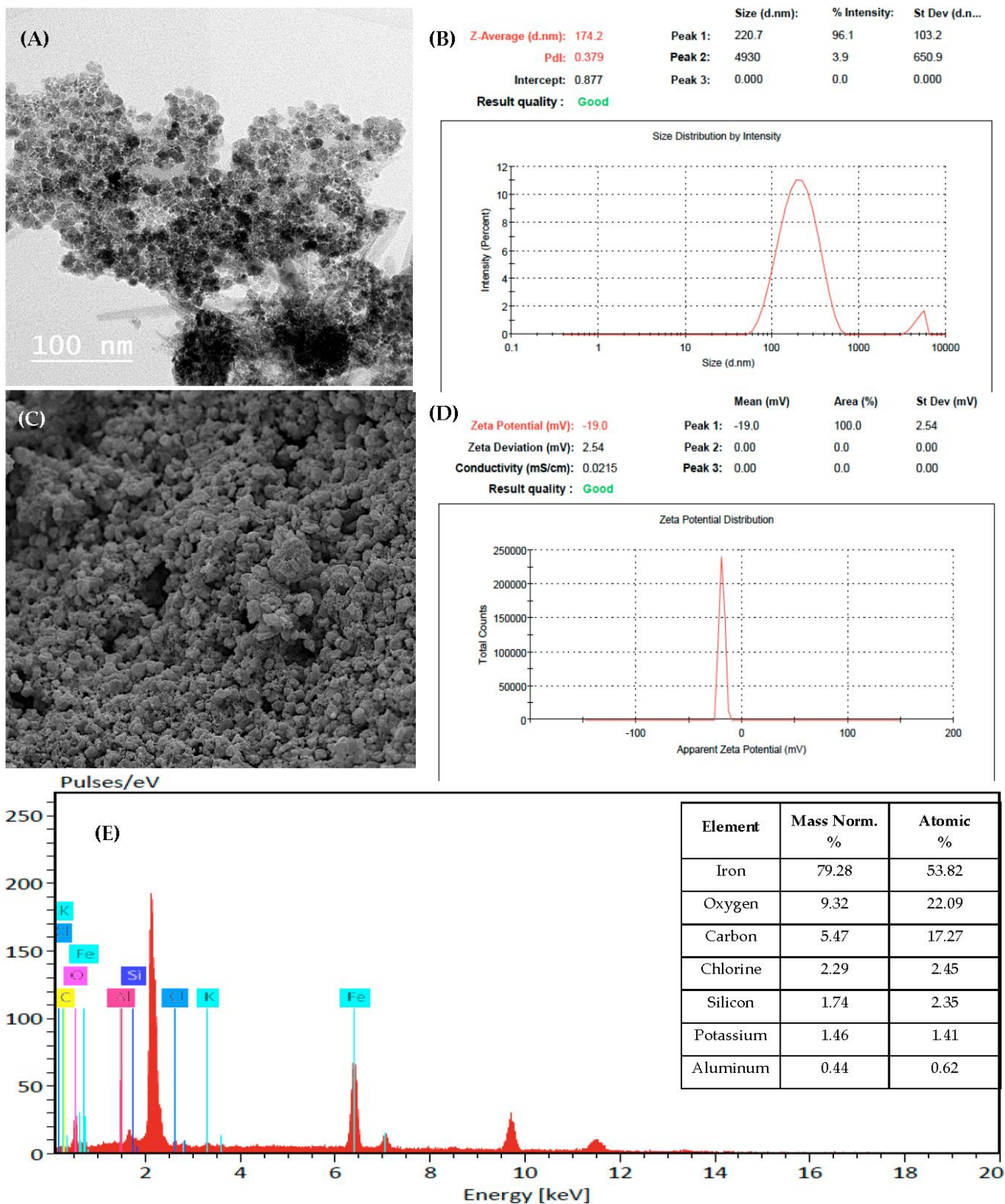


**Figure 1.** TEM image (A), Zeta average diameter (B), SEM image (C), Zeta potential (D) and EDX profile of Fe<sub>3</sub>O<sub>4</sub>/HA NPs (E).

### 3.2. Inhibitory Effect of Fe<sub>3</sub>O<sub>4</sub>/HA NPs on the Mycelial Growth of *A. striticum*

Three used concentrations, 10, 40, and 80 mg L<sup>-1</sup>, of Fe<sub>3</sub>O<sub>4</sub>/HA NPs inhibited the mycelial growth of *A. striticum* in comparison to the controls (Figure 2A). The highest inhibition rate was observed at 80 mg L<sup>-1</sup> concentration, with value of 62.22%, followed

by  $40 \text{ mg L}^{-1}$  concentration, with a value of 44.44% (Figure 2B). The least inhibition rate 16.67% was observed at a  $10 \text{ mg L}^{-1}$  concentration (Figure 2B).

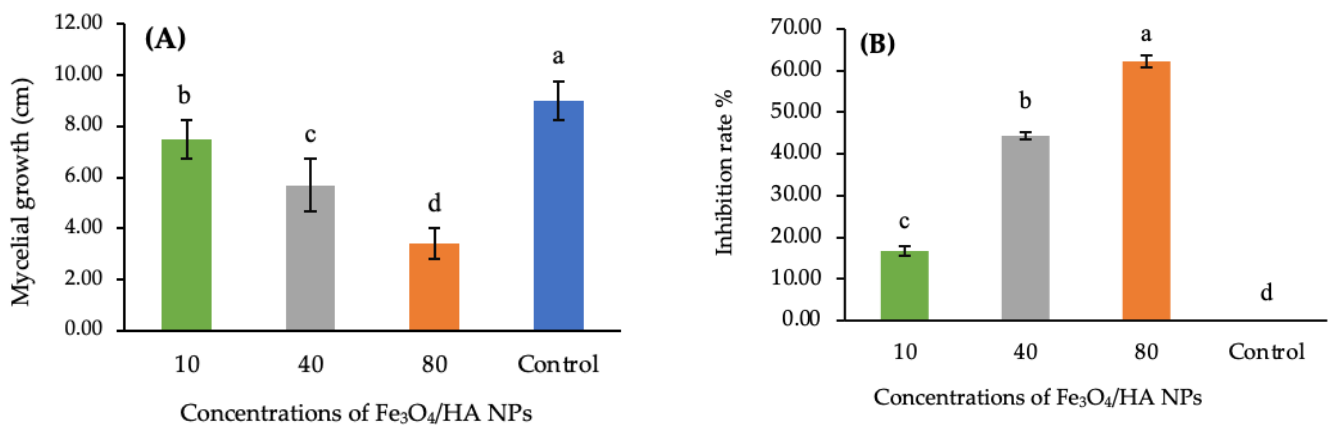


**Figure 2.** Inhibitory effect of Fe<sub>3</sub>O<sub>4</sub>/HA NPs on the mycelial growth of *A. striticum* (A) and inhibition rate (B). Same letter in the figure means no significant differences between the values.

### 3.3. Reaction of Grain Sorghum Genotypes to Acremonium Wilt Disease

All tested twenty-one sorghum genotypes responded differently to *A. striticum* infection. The infected plants developed reddish to dark brown vascular bundles and stalks after 90 days of sowing. The disease rating was quantified based on their response to wilt disease and the disease severity index (DSI) and infection percent were calculated. All the genotypes were categorized into six groups, ranging from highly susceptible to highly resistant genotypes. The first group consisted of four highly resistant genotypes: LG 13, Local 119, Dorado, and LG 23. The second group was of moderately resistant genotypes and included Line c, H 301, local 129, and ICSR 93002 genotypes. The third group was the largest group and comprised of nine resistant genotypes: Assuit 14, Local 245, Sel 1007, LG 35, LG 47, H sh 1, H 304, H305, and ICSR 92003. Only one genotype (LG 3) was found to be moderately susceptible in the fourth group. Giza 3 and Giza 113 were two susceptible genotypes in the fifth group. Only one genotype, LG 1, constituted the sixth group and was highly susceptible (Table 3).

### 3.4. Effect of Fe<sub>3</sub>O<sub>4</sub>/HA NPs on Controlling Acremonium Wilt under Field Conditions

The effects of synthesized NPs on the severity of acremonium wilt on five sorghum genotypes were studied over two consecutive seasons (Table 4). The DR of the five tested genotypes was comparable in the two seasons. Nonetheless, the DR differed significantly ( $p \leq 0.05$ ) at the different concentrations of Fe<sub>3</sub>O<sub>4</sub>/HA NPs. The highest DSIs were observed at  $10 \text{ mg L}^{-1}$  concentration, and a concentration of  $80 \text{ mg L}^{-1}$  yielded the best control efficacy. Local 119, a highly resistant genotype, demonstrated the highest efficacy of 80% against *A. striticum*. Moreover, the concentrations 40 and  $80 \text{ mg L}^{-1}$  showed a great efficacy in controlling acremonium wilt on LG 1 (highly susceptible) and Giza 3 (susceptible) genotypes during the two seasons.

**Table 3.** Reaction of twenty-one grain sorghum genotypes for acremonium wilt disease during season 2019.

No.	Genotypes	DR ± St.Dev.	Group Type
1	LG 13	0.17 ± 0.03	HR
2	Assuit 14	0.67 ± 0.10	R
3	Line c	1.11 ± 0.10	MR
4	Local 119	0.52 ± 0.08	HR
5	Local 245	0.72 ± 0.04	R
6	Dorado	0.39 ± 0.01	HR
7	LG 23	0.46 ± 0.07	HR
8	Sel 1007	0.83 ± 0.04	R
9	LG 35	0.89 ± 0.10	R
10	LG 47	0.73 ± 0.03	R
11	H sh 1	0.72 ± 0.05	R
12	H 301	1.25 ± 0.06	MR
13	H 305	0.90 ± 0.04	R
14	H 306	0.93 ± 0.02	R
15	LG 1	4.12 ± 0.11	HS
16	Giza 3	3.45 ± 0.22	S
17	Giza 113	3.06 ± 0.13	S
18	Local 129	1.29 ± 0.08	MR
19	ICSR 92003	1.02 ± 0.08	R
20	ICSR 93002	1.08 ± 0.08	MR
21	LG 3	2.03 ± 0.06	MS
	Average	1.25	
	LSD 0.05	0.14	

Abbreviations used in the table are: the least significant difference (LSD), highly susceptible (HS), moderately susceptible (MS), susceptible (S), resistant (R), moderately resistant (MR), and highly resistant (HR), standard deviation (St.Dev.) and disease rating (DR).

**Table 4.** Effect of Fe<sub>3</sub>O<sub>4</sub>/HA NPs on acremonium wilt of grain sorghum during seasons 2020 and 2021.

Genotypes	Concentration (mg L <sup>-1</sup> )	Season 2020		Season 2021	
		DR ± St.Dev.	Efficacy (%)	DR ± St.Dev.	Efficacy (%)
Giza 113	10	3.2 ± 0.20	17.3	3.53 ± 0.15	7.8
	40	1.8 ± 0.10	53.49	1.87 ± 0.25	51.17
	80	1.53 ± 0.06	60.47	1.5 ± 0.30	60.84
	Control	3.87 ± 0.15	-	3.83 ± 0.21	-
LG 1	10	3.3 ± 0.20	22.72	3.37 ± 0.31	22.25
	40	1.73 ± 0.15	59.48	1.83 ± 0.06	57.74
	80	1.2 ± 0.10	71.9	1.23 ± 0.06	71.59
	Control	4.27 ± 0.06	-	4.33 ± 0.25	-
LG 3	10	2.03 ± 0.06	2.4	2.5 ± 0.20	8.42
	40	1.3 ± 0.10	37.2	1.23 ± 0.06	54.95
	80	0.97 ± 0.21	53.14	0.9 ± 0.17	67.03
	Control	2.07 ± 0.31	-	2.73 ± 0.31	-
Giza 3	10	2.93 ± 0.12	14.0	2.77 ± 0.21	20.17
	40	1.47 ± 0.06	58.82	1.4 ± 0.10	59.65
	80	1.1 ± 0.20	69.19	0.97 ± 0.12	72.04
	Control	3.57 ± 0.25	-	3.47 ± 0.15	-
Local 119	10	0.37 ± 0.06	26.0	0.4 ± 0.10	20.0
	40	0.13 ± 0.06	74.0	0.13 ± 0.06	74.0
	80	0.1 ± 0.00	80.0	0.1 ± 0.00	80.0
	Control	0.5 ± 0.10	-	0.5 ± 0.00	-
LSD of treatments		0.11		0.48	
LSD of genotypes		0.18		0.53	

Abbreviations used in the table are standard deviation (St.Dev.) and disease rating (DR).

### 3.5. Effect of Fe<sub>3</sub>O<sub>4</sub>/HA NPs on the Growth and Yield of Grain Sorghum

Plant heights, grain weight and yield differed significantly ( $p < 0.05$ ) among five genotypes in response to different concentrations of Fe<sub>3</sub>O<sub>4</sub>/HA NPs (Tables 5–7). The concentration of 40 mg L<sup>-1</sup> was the most effective in increasing plant height, as compared to the other concentrations, with the highest plant height recorded in the two seasons being 390.33 and 392.33 cm for the Local 119 genotype, respectively (Table 5). The highest mean value of plant height for all the five genotypes was 382.67 cm in season 2020 and 377.27 cm in the season 2021.

**Table 5.** Effect of Fe<sub>3</sub>O<sub>4</sub>/HA NPs on plant height of grain sorghum during the seasons of 2020 and 2021.

Concentration (mg L <sup>-1</sup> )	Plant Height (cm)											
	Season 2020						Season 2021					
	Giza 113	LG 1	LG 3	Giza 3	Local119	Mean	Giza 113	LG 1	LG 3	Giza 3	Local119	Mean
10	370.33	363.00	355.33	375.00	376.67	368.07	371.67	362.67	353.50	373.44	375.67	367.39
40	386.00	377.00	371.33	388.67	390.33	382.67	382.67	370.00	360.00	381.33	392.33	377.27
80	311.00	307.33	297.33	318.67	325.67	312.00	309.37	300.14	291.33	315.47	324.67	308.20
Control	370.33	360.33	353.33	371.33	375.33	366.13	370.67	361.44	350.00	372.00	375.00	365.82
Mean	359.42	351.92	344.33	363.42	367.00	357.22	358.59	348.56	338.71	360.56	366.92	354.67
	F test			LSD at 0.05			F test			LSD at 0.05		
Treatments	**			3.17			**			3.57		
Genotypes	**			2.00			**			2.71		
Interaction				NS						NS		

\*\* means significant 5% at level of probability.

**Table 6.** Effect of Fe<sub>3</sub>O<sub>4</sub>/HA NPs on the 1000-grain weight of grain sorghum during the seasons of 2020 and 2021.

Concentration (mg L <sup>-1</sup> )	1000-Grain Weight (g)											
	Season 2020						Season 2021					
	Giza 113	LG 1	LG 3	Giza 3	Local119	Mean	Giza 113	LG 1	LG 3	Giza 3	Local119	Mean
10	42.45	36.60	38.55	40.47	41.74	39.96	40.78	36.00	39.89	42.89	41.90	40.29
40	45.31	38.07	40.55	43.27	44.32	42.31	43.35	38.30	42.60	44.34	45.08	42.73
80	32.86	27.82	30.39	31.69	34.91	31.53	32.29	26.43	30.26	31.29	33.05	30.66
Control	42.22	36.20	38.27	40.26	41.50	39.69	40.50	35.73	39.03	42.75	41.34	39.87
Mean	40.71	34.67	36.94	38.92	40.62	38.37	39.23	34.12	37.95	40.32	40.34	38.39
	F test			LSD at 0.05			F test			LSD at 0.05		
Treatments	**			1.3			**			0.84		
Genotypes	**			1.08			**			0.6		
Interaction				NS						1.2		

\*\* mean significant 5% at level of probability.

The genotypes Giza 113 and Local 119 treated with 40 mg L<sup>-1</sup> exhibited a substantial increase in the weight of 1000 grains. The highest mean value of 1000 grain weight treated with the concentration of 40 mg L<sup>-1</sup> was 42.31 g and 42.73 g in the seasons 2020 and 2021, respectively (Table 6). Furthermore, the concentration of 40 mg L<sup>-1</sup> had the greatest impact on the grain yield/plant for all the genotypes, with Giza 113 and Local 119 scoring the highest, with 84.10 g and 83.96 g for the season 2020 and 83.25 and 85.84 g for the season 2021. The LSD test ( $p < 0.05$ ), however, revealed a low significant difference in the mean values of treatments and genotypes in terms of yield/plant. Conversely, no significant difference was observed in their interaction. The highest concentration, 80 mg L<sup>-1</sup>, had a distinct negative impact on the plant heights, 1000-grain weight and yield attributes (Tables 5–7).

**Table 7.** Effect of Fe<sub>3</sub>O<sub>4</sub>/HA NPs on the grain yield/ plant for grain sorghum plants during the seasons of 2020 and 2021.

Concentration (mg L <sup>-1</sup> )	Grain Yield/Plant (g)											
	Season 2020						Season 2021					
	Giza 113	LG 1	LG 3	Giza 3	Local119	Mean	Giza 113	LG 1	LG 3	Giza 3	Local119	Mean
10	79.41	71.51	73.05	74.81	80.93	75.94	78.71	71.89	72.68	75.51	81.86	76.13
40	84.10	74.44	75.64	76.59	83.96	78.95	83.25	73.67	75.91	79.04	85.54	79.48
80	70.81	62.54	60.88	65.01	71.82	66.21	67.72	62.16	59.61	61.69	70.57	64.35
Control	79.09	71.30	73.17	74.18	80.29	75.60	78.36	71.67	72.49	75.16	81.48	75.83
Mean	78.35	69.95	70.68	72.65	79.25	74.18	77.01	69.85	70.17	72.85	79.86	73.95
	F test			LSD at 0.05			F test			LSD at 0.05		
Treatments	**			0.77			**			0.98		
Genotypes	**			1.11			**			0.62		
Interaction	NS			NS			NS			1.25		

\*\* mean significant 5% at level of probability.

### 3.6. Effect of Fe<sub>3</sub>O<sub>4</sub>/HA NPs on the Level of Gibberellic Acid in Grain Sorghum Genotypes

A concentration of 40 mg L<sup>-1</sup> of Fe<sub>3</sub>O<sub>4</sub>/HA NPs led to a significant ( $p < 0.05$ ) increase in the level of gibberellic acid (GA3) in five sorghum genotypes. In contrast, the concentration of 80 mg L<sup>-1</sup> significantly ( $p < 0.05$ ) downregulated the level of GA3 in all the genotypes when compared to the control and the lowest concentration of 10 mg L<sup>-1</sup>. GA3 levels remained unaffected by the lowest concentration, 10 mg L<sup>-1</sup>, and were comparable to untreated control plants (Figure 3).

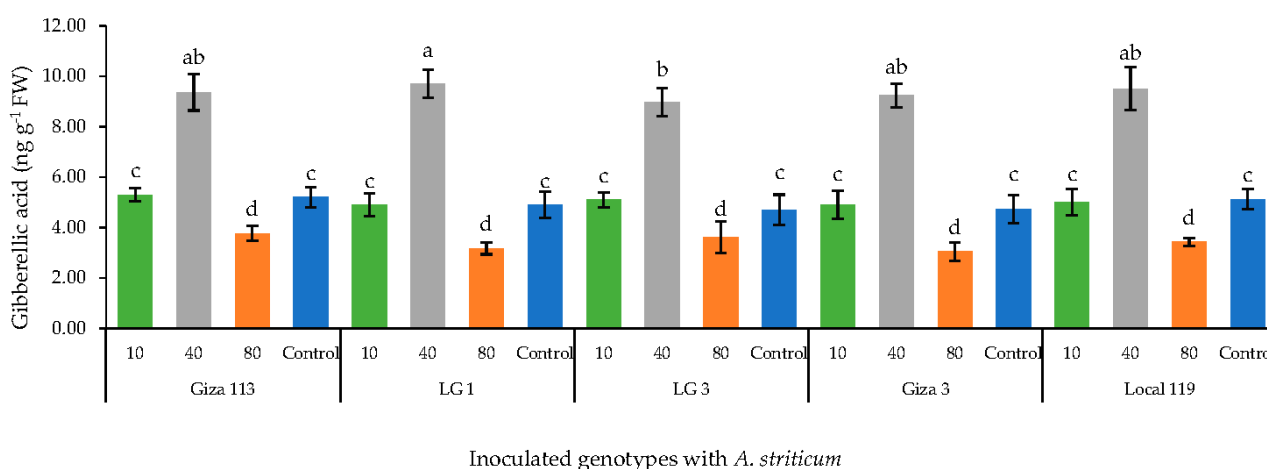


**Figure 3.** Effect of Fe<sub>3</sub>O<sub>4</sub>/HA NPs on the level of gibberellic acid (GA3) in grain sorghum genotypes. Same letter in the figure means no significant differences between the values.

### 3.7. Effect of Fe<sub>3</sub>O<sub>4</sub>/HA NPs on the Activity of Peroxidase and Catalase Enzymes in Grain Sorghum

The five sorghum genotypes treated with either 40 mg L<sup>-1</sup> or 80 mg L<sup>-1</sup> concentration of Fe<sub>3</sub>O<sub>4</sub>/HA NPs showed a significant ( $p < 0.05$ ) increase in the enzymatic activity of peroxidase and catalase in healthy (uninoculated) plants in comparison with the infected plants (Figures 4A and 5A). Notably, no significant increase in the activities of both enzymes were noted in infected sorghum genotypes.

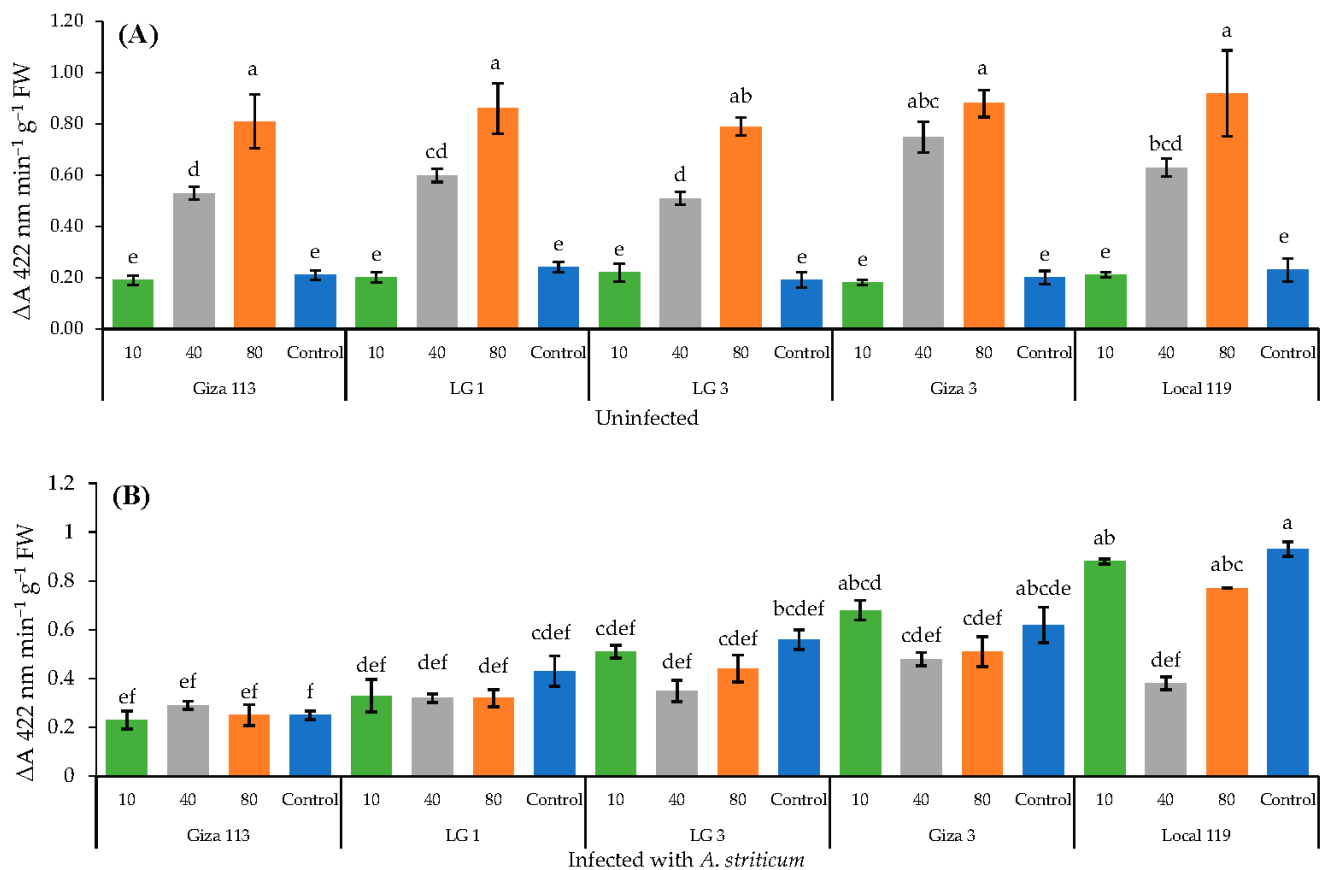


**Figure 4.** Activity of peroxidase in grain sorghum plants uninfected (A) and infected with *A. striticum* (B) in response to application of Fe<sub>3</sub>O<sub>4</sub>/HA NPs. Same letter in the figure means no significant differences between the values.

The peroxidase activities of two genotypes, LG 3 and Giza 3, were comparable to each other in response to different concentrations of Fe<sub>3</sub>O<sub>4</sub>/HA NPs (Figure 4B). The peroxidase activity of all the five genotypes decreased substantially at concentrations of 40 and 80 mg L<sup>-1</sup> in infected plants as compared to healthy plants (Figure 4B). Nonetheless, a variable trend was observed at 10 mg L<sup>-1</sup> and in control plants. Two genotypes, Giza 3 and Local 119, showed a significant ( $p < 0.05$ ) increase in peroxidase activity at a concentration of 10 mg L<sup>-1</sup> and in control plants (Figure 4B).

Catalase activity was significantly reduced in all infected sorghum genotypes treated with 40 and 80 mg L<sup>-1</sup> NP concentrations (Figure 5B). On the other hand, the catalase activity enhanced in infected sorghum plants treated with 10 mg L<sup>-1</sup> as compared to healthy (uninfected) control plants (Figure 5B). Nonetheless, a highest increase in the catalase activity was noted in the Giza 3 and Local 119 genotypes (Figure 5B).

### 3.8. Potential Toxicity of Fe<sub>3</sub>O<sub>4</sub>/HA NPs in Rats

Hematological examinations of rats fed with grain sorghums treated with different concentrations of Fe<sub>3</sub>O<sub>4</sub>/HA NPs did not show any significant difference until 36 days of feeding. Likewise, no significant increase in the red blood cells (RBCs) count was observed at 36 days of post-feeding, but the hemoglobin (Hb) level significantly increased ( $p < 0.05$ ) at 36 days and continued to increase at 51 days at 40 and 80 mg L<sup>-1</sup> concentrations. However, at 51 days of post feeding, a significant increase in the RBCs count was observed at 40 and 80 mg L<sup>-1</sup> concentrations (Table 8).

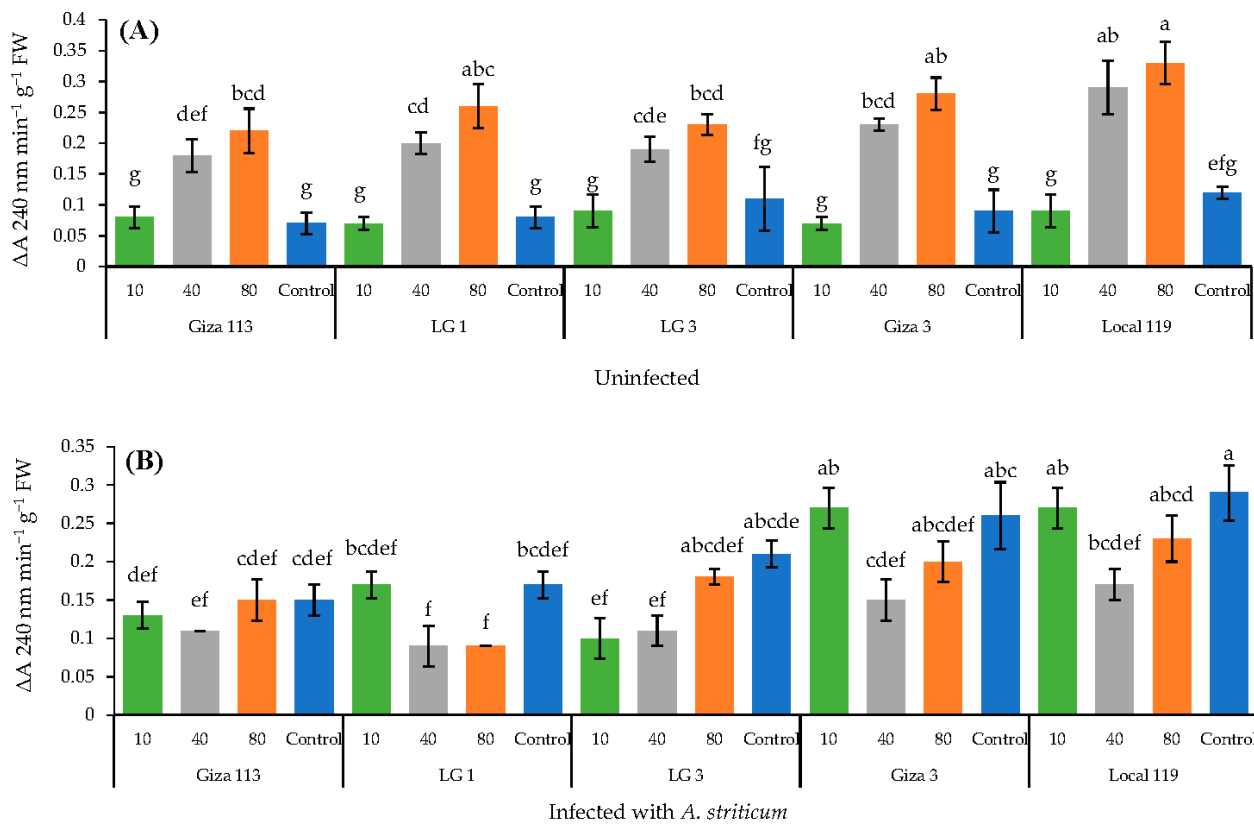


**Figure 5.** Activity of catalase in grain sorghum plants uninfected (A) and infected with *A. striticum* (B) in response to application of Fe<sub>3</sub>O<sub>4</sub>/HA NPs. Same letter in the figure means no significant differences between the values.

**Table 8.** Hematological attributes of male albino rats fed on grain sorghum treated with Fe<sub>3</sub>O<sub>4</sub>/HA NPs.

Days after Feeding	Concentration (mg L <sup>-1</sup> )	CBC Analysis		
		RBCs (10 <sup>6</sup> )	WBCs (10 <sup>3</sup> )	Hb (mg dL <sup>-1</sup> )
21	10	7.63	6.83	14.2
	40	7.47	7.43	14.1
	80	7.5	7.6	14.5
	Control	7.42	7.57	14.1
36	10	7.52	7.32	14.63
	40	7.72	7.83	14.78
	80	7.8	7.6	15
	Control	7.38	7.08	14.5
51	10	7.87	7.15	14.49
	40	8.29	7	15.3
	80	8.88	7.5	16.1
	Control	7.49	7.25	14.4
LSD 0.05 Treatment		0.54	0.52	0.4
LSD 0.05 Days of feed		0.47	0.45	0.35

Abbreviation used in the table are complete blood count (CBC), white blood cells (WBCs), red blood cells (RBCs), and hemoglobin (Hb).

The enzymatic activity of alanine aminotransferase (ALT) and aspartate aminotransferase (AST) was used to assess the liver function of rats feeding on grain sorghums treated with different concentrations of Fe<sub>3</sub>O<sub>4</sub>/HA NPs (Table 9). From 21 to 51 days of feeding, rats fed on 80 mg L<sup>-1</sup> concentration experienced a gradual increase in ALT levels, whereas the level of AST was not highly affected as compared to the control.

**Table 9.** Liver and kidney functions analysis of male albino rats fed on grain sorghum treated with Fe<sub>3</sub>O<sub>4</sub>/HA NPs.

Days after Feeding	Concentration (mg L <sup>-1</sup> )	Blood Chemistry		
		AST (u L <sup>-1</sup> )	ALT (u L <sup>-1</sup> )	Creatinine (mg dL <sup>-1</sup> )
21	10	79	34.4	0.57
	40	83	36.7	0.57
	80	86	57.2	0.6
	Control	80	33.5	0.58
36	10	85	35	0.6
	40	84.6	38	0.59
	80	86	65.7	0.61
	Control	84	34.5	0.6
51	10	83.8	35	0.67
	40	84.3	40.7	0.69
	80	85	80.3	0.88
	Control	83	35	0.66
LSD 0.05 Treatment		0.88	0.88	0.07
LSD 0.05 Days of feed		0.76	0.76	0.06

The level of creatinine remained unaffected by all concentrations when compared to the control until 36 days of feeding. However, after 51 days, there was a marked increase in the creatinine level in the rats feeding on 80 mg L<sup>-1</sup> concentration of Fe<sub>3</sub>O<sub>4</sub>/HA NPs which recorded 0.88 mg dL<sup>-1</sup>, but this did not indicate kidney failure (Table 9).

#### Histopathological Examination

No morphological changes were observed in the hepatic parenchyma of rats administered with untreated grain sorghums or grain sorghums treated with 10 mg L<sup>-1</sup> of Fe<sub>3</sub>O<sub>4</sub>/HA NPs (Figure 6A,B). The kidneys of these rats showed no histopathological changes in the glomeruli and tubules at the cortex (Figure 7A,B), whereas the hepatic parenchyma of rats administered with 40 mg L<sup>-1</sup> of Fe<sub>3</sub>O<sub>4</sub>/HA NP-treated grain sorghums exhibited mild pathological changes in the portal areas, including inflammatory cells infiltrations and portal vein dilatations (Figure 6C). The kidneys of these rats showed a few focal inflammatory cells infiltration between the sclerotic dilated blood vessels, glomeruli and tubules (Figure 7C). The hepatic parenchyma of rats administered with grain sorghums treated with 80 mg L<sup>-1</sup> of Fe<sub>3</sub>O<sub>4</sub>/HA NPs showed several pathological alterations, such as massive inflammatory cells' infiltration between the fatty changed hepatocytes all over the parenchyma (Figure 6D). Furthermore, histopathological alterations, such as focal massive inflammatory cell aggregation in between the degenerated necrosis tubules and vacuolization in the endothelial cells lining the glomeruli, were clearly observed in the kidneys of these rats (Figure 7D).

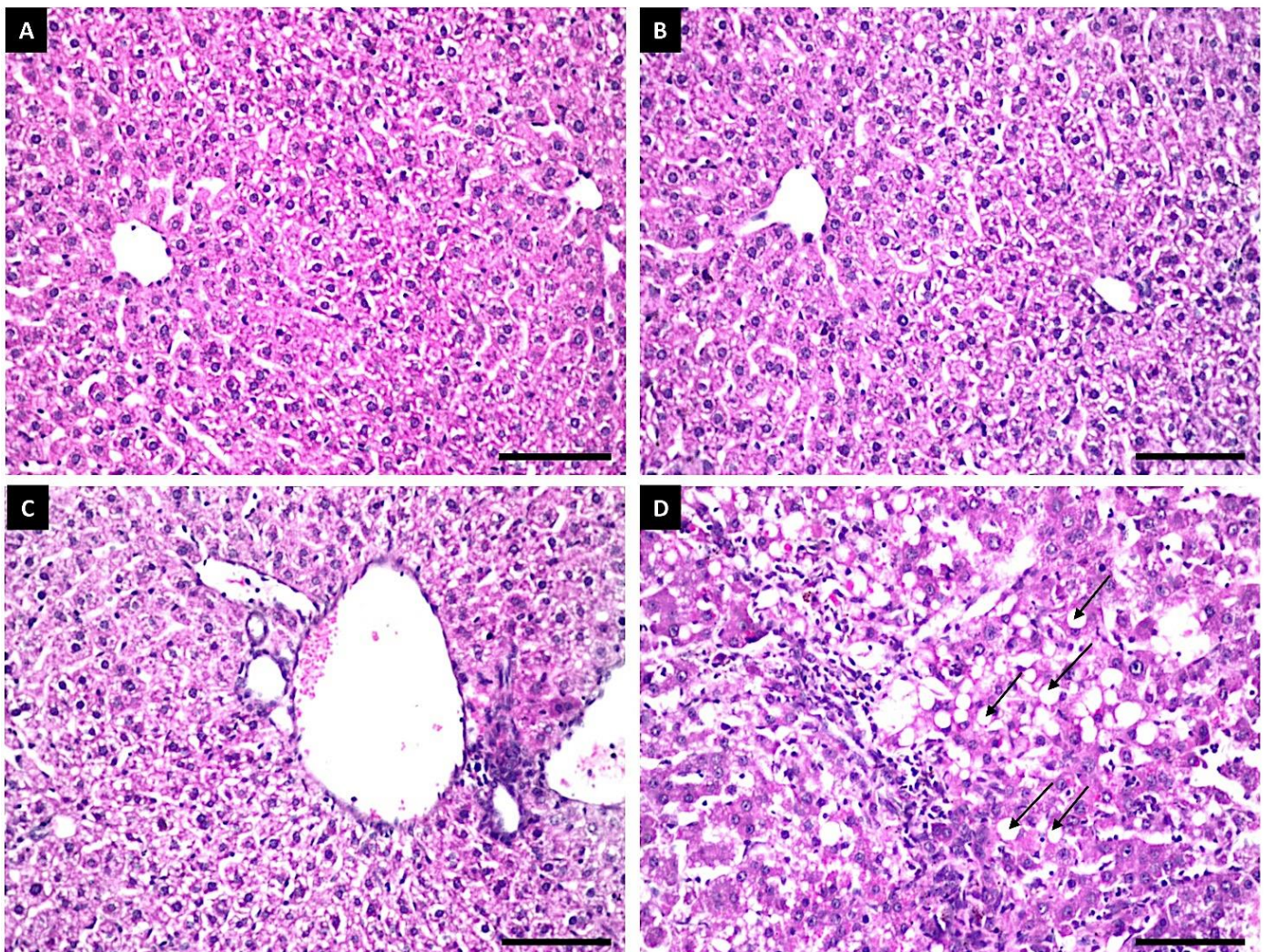


**Figure 6.** Histopathological changes in the livers of male albino rats fed with grain sorghums treated with  $\text{Fe}_3\text{O}_4/\text{HA}$  NPs; no histopathological changes were recorded in the hepatocytes and central vein of control (untreated) and treated with  $10 \text{ mg L}^{-1}$  rats (**A,B**); few inflammatory cells infiltration and dilatation in the portal vein of rats exposed to  $40 \text{ mg L}^{-1}$   $\text{Fe}_3\text{O}_4/\text{HA}$  NPs (**C**); massive inflammatory cells infiltration was detected in between the fatty changed hepatocytes all over the parenchyma (black arrow) of rats exposed to  $80 \text{ mg L}^{-1}$   $\text{Fe}_3\text{O}_4/\text{HA}$  NPs (**D**). Scale bar represents  $100 \mu\text{m}$ .

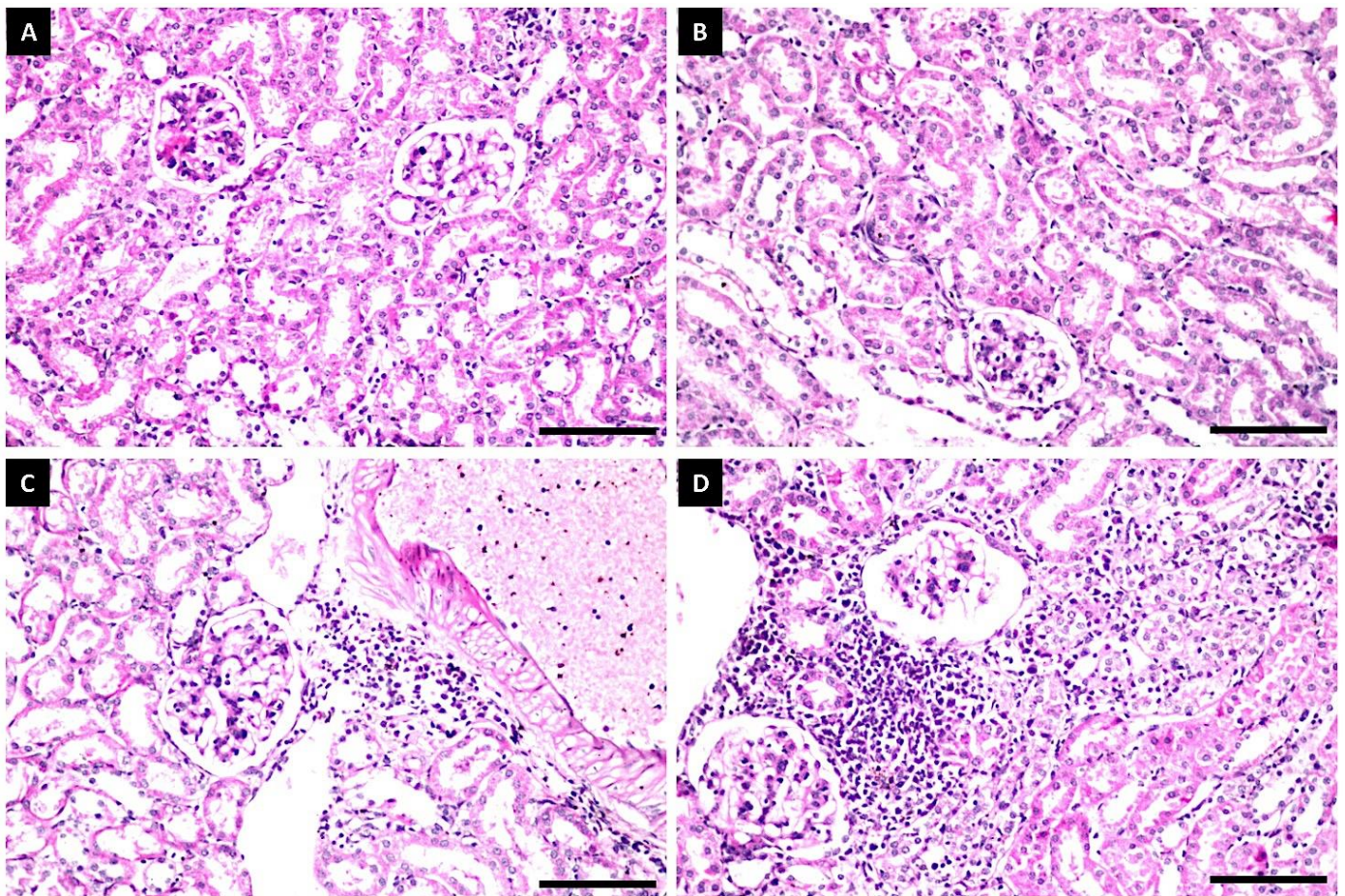


**Figure 7.** Histopathological changes in the kidney of male albino rats fed with grain sorghums treated with  $\text{Fe}_3\text{O}_4/\text{HA}$  NPs; no histopathological alteration in the glomeruli and tubules at the cortex were recorded in untreated and treated rats with  $10 \text{ mg L}^{-1}$  (A,B); few focal inflammatory cells infiltration was detected in between the sclerotic dilated blood vessels, glomeruli and tubules of rats exposed to  $40 \text{ mg L}^{-1}$   $\text{Fe}_3\text{O}_4/\text{HA}$  NPs (C); focal massive inflammatory cell aggregation in between the degenerated necrosis tubules as well as vacuolization in the endothelial cells lining the glomeruli of rats exposed to  $80 \text{ mg L}^{-1}$   $\text{Fe}_3\text{O}_4/\text{HA}$  NPs (D). Scale bar represents  $100 \mu\text{m}$ .

#### 4. Discussion

The current study was the first to investigate the inhibitory effect of  $\text{Fe}_3\text{O}_4/\text{HA}$  NPs against a fungal pathogen, *A. striticum*. The TEM and SEM images confirmed the spherical shape of  $\text{Fe}_3\text{O}_4/\text{HA}$  [34], with sizes ranged from 60–72 nm. However, the hydrodynamic size obtained through DLS (Figure 1B) was larger (174 nm) than the size obtained through TEM. These findings corroborate an earlier report wherein the different sizes of iron oxide NPs were observed [54]. The average size distribution of  $\text{Fe}_3\text{O}_4/\text{HA}$  NPs in colloids was 174 nm, representing 96% of all colloidal solution, which is in agreement with the previous findings [32] and contrasted to another where size of NPs were 239 nm [19]. Iron oxide NPs usually range from 1 to 100 nm in size, but the higher size observed here may likely be due to the HA coating. Moreover, the Pdi recorded 0.379, indicating moderate polydispersity which is in close proximity with previously recorded 0.423 Pdi [55]. The zeta potential was  $-19.0 \text{ mV}$ , indicating that  $\text{Fe}_3\text{O}_4/\text{HA}$  NPs have a hydrodynamic diameter in the nanoscale which is similar to previously reported [40].

Different concentrations 10, 40 and  $80 \text{ mg L}^{-1}$  of  $\text{Fe}_3\text{O}_4/\text{HA}$  NPs significantly ( $p < 0.05$ ) reduced the mycelial growth of *A. striticum* over the control. Our finding is supported by earlier studies that exhibited the antimicrobial activity of  $\text{Fe}_3\text{O}_4$  and HA against fungal and bacterial agents [56–61]. Iron oxide NPs have not only been shown to boost the plant growth

but also exhibit the antifungal activities against a variety of fungal pathogens [58]. In the poisoned food technique, iron NPs inhibited the mycelial growth of *Alternaria alternata* up to 87.9% at a  $1.0 \text{ mg mL}^{-1}$  concentration [62]. Iron oxide NPs exhibited significant antimycotic activity against *Aspergillus niger* and *Mucor piriformis*, but were more active against *Mucor piriformis* [63], inhibited *Trichothecium roseum* spore germination (up to 87.74%) and *Cladosporium. herbarum* (up to 84.89%) [56]. The foliar spray and soil application of iron NPs improved the morpho-physiochemical attributes, morphological traits (sprouting percentage, number of leaves, plant biomass, root attributes), and biochemical attributes (such as chlorophyll, sugar content, and enzymatic activity of antioxidants) [54]. HA has been shown to have antimicrobial activity against a variety of pathogenic bacteria [64] and fungi, including *Botrytis cinerea*, *Fusarium graminearum*, *Phylospora piricola*, *Phytophthora infestans*, *Rhizoctonia cerealis*, and *Sclerotinia sclerotiorum* [65,66]. The exact mechanisms underlying the antifungal activity of  $\text{Fe}_3\text{O}_4$ /HA NPs need to be investigated and could be the subject of futuristic studies. However, antifungal activity could be accredited to either iron oxide or HA or could be a combined effect of these two. Previous studies have bounded the antimicrobial activity of iron oxide NPs to their extremely tiny size and larger surface area, which reduces oxygen supply for respiration [67] or causes cell damage due to the oxidative stress generated by reactive oxygen species, ultimately leading to the inhibition of microbial growth [57,68–70]. Furthermore, iron reacts with oxygen to create hydrogen peroxide, which then reacts with ferrous ions to form hydroxyl radicals that disrupt the cell components [71]. On the other side, HA controls plant diseases by inducing systemic acquired resistance [72], or by inhibiting the growth of microorganisms due to its unique chemical composition and functional group (COOH) properties [73].

The screened sorghum genotypes responded variably to acremonium wilt. At present, few works have been performed on the screening of sorghum genotypes against acremonium wilt under Egyptian conditions. Available studies in Egypt reported that the hybrids H-301 and H-302 were resistant to acremonium wilt disease, and stated that the genotype Giza 15 (Egyptian) was susceptible and Dorado (USA) was resistant [44,74]. Fortunately, this work provides an advance for the wide screening of for 21 sorghum genotypes, and thus represents a useful datum for researchers in the future.

The phenotypic traits of sorghum genotypes showed dramatic effects on the resulting plants' growth and yield upon exposure to the  $\text{Fe}_3\text{O}_4$ /HA treatments. The genotypes treated with  $40 \text{ mg L}^{-1}$  revealed longer shoots and higher yield. No significant changes were observed in the growth and yield of sorghum genotypes treated either with  $10 \text{ mg L}^{-1}$  or untreated control. It is well known that iron is a very important trace element for photosynthetic processes and plant growth. Many investigators pointed out the significant effect of iron on the growth, yield and other biochemical parameters of many plants [75,76]. Along with this, Li et al. demonstrated that foliar spraying with suitable concentrations ( $20\text{--}50 \text{ mg L}^{-1}$ ) of iron oxide NPs could significantly promote the growth of *P. heterophylla* and increase the root yield per unit area under field conditions [77]. In fact, the higher concentration  $80 \text{ mg L}^{-1}$  caused a negative effect on the growth of all genotypes. Other studies reported similar results where they found out that the high concentrations of  $\text{Fe}_3\text{O}_4$  NPs had an inhibitory effect on growth due to accumulation in some cells, leading to stress effects [77,78]. The importance of HA cannot be ignored as many studies explored its beneficial application as biological amendments for maintaining plant growth [79–82].

Several studies have shown that NP applications increased the activity of different antioxidant enzymes such as catalase, superoxide dismutase and peroxidase [82–84]. As per our findings, the stimulating effect of  $\text{Fe}_3\text{O}_4$ /HA NPs was directly proportional to their tested concentrations. The higher concentrations of 40 and  $80 \text{ mg L}^{-1}$  increased the activity of peroxidase and catalase in non-infected plants compared to the infected one. Despite stimulating the activity of oxidative enzymes, the higher concentration of  $80 \text{ mg L}^{-1}$  negatively affected the growth of sorghum genotypes. However, Haydar et al. noted that the activities of all studied enzymes except peroxidase increased along with the

plant growth [54]. The dissimilarities in published results might be due to the difference in NP size, culture condition or plant species used in the studies [77].

The current study's goal was to assess the potential toxicity of Fe<sub>3</sub>O<sub>4</sub>/HA NPs in male albino rats via assessing any changes in complete blood count (CBC), liver and kidney functions and their histological features. Biocompatibility and the potential impact of nanomaterials and polymers on the immune system of model animals and on immune-related hematological parameters have been explored [85–87]. The results of the current study indicated that the administration of lower concentrations 10 mg L<sup>-1</sup> was not associated with histopathological changes neither in the liver nor in the kidney and no significant changes in liver enzymes were recorded. This is consistent with the findings that lower doses of Fe<sub>3</sub>O<sub>4</sub> had no negative effects on liver tissues and enzymes [86,88]. Moreover, the magnetic NPs of 50 nm size did not cause apparent toxicity under the experimental conditions [89]. Compared to unexposed control, the tested concentrations of chitosan-coated iron oxide NPs had no effect on the creatinine level in rats and did not create any toxicity in the kidney [90]. These findings confirm that lower doses have good biocompatibility in mice. However, in this study, administration to a higher dose 40 mg L<sup>-1</sup> revealed mild histopathological effects on liver and kidney. The higher dose 80 mg L<sup>-1</sup>-induced histopathological alterations in the kidney and liver as well as increased the level of ALT and creatinine after 51 days of feeding. This increment might be due to AST and ALT leakage from the liver cytosol to blood flow and led to an increase in their activities [91,92]. Thus, AST and ALT enzyme are markers for liver damage, confirmed by our histopathological findings (fatty changed hepatocytes all over the parenchyma). Thus, the increase in the ALT enzyme shows the damaging effect of iron oxide NPs on liver cells. These findings are supported with those reported earlier. The possible reasons that can explain these conflicting reports include the physicochemical properties of the NPs, such as shape, size and solubility. Additionally, experimental conditions, exposure time and doses can cause variation in results [93].

## 5. Conclusions and Further Perspectives

The use of nanomaterials in agriculture, especially nanofertilizers having antimycotic properties, could pave the way for smart agriculture. The current study significantly adds new information and yielded promising results about the antimycotic and biofertilizer effects of Fe<sub>3</sub>O<sub>4</sub>/HA NPs. It was shown that the concentrations of 40 and 80 mg L<sup>-1</sup> had a great efficacy in controlling the causal agent of acremonium wilt in vivo and in vitro. Unfortunately, the higher concentrations had a negative impact on the activities of peroxidase and catalase enzymes in infected sorghum plants. Only a concentration of 40 mg L<sup>-1</sup> was the most effective in increasing the gibberellic acid level as well as the growth of grain sorghum plants. Conclusively, Fe<sub>3</sub>O<sub>4</sub>/HA NPs at a concentration of 40 mg L<sup>-1</sup> could be regarded as safe and could potentially be opted in agriculture applications against the filamentous fungus *A. strictum*. However, the molecular mechanisms underlying Fe<sub>3</sub>O<sub>4</sub>/HA NPs-mediated antimycotic mechanisms needs further investigation and could be a subject of futuristic studies. Furthermore, the application of iron oxide NPs in agriculture reveals one more issue: utilizing Fe<sub>3</sub>O<sub>4</sub>/HA NPs showed some limitations at a higher dose of 80 mg L<sup>-1</sup>. Therefore, the application of Fe<sub>3</sub>O<sub>4</sub>/HA NPs still requires more effort to achieve the hope for the future. These efforts might focus on the use of alternative coating materials and stabilizing the surface of iron oxide NPs in order to reduce toxicity and increase biocompatibility.

**Author Contributions:** Conceptualization, A.M.E.-B., A.Z.E.-A., A.A.E.A., A.M.I., H.M.H., H.S.E.-B., O.A.Y.A.E. and Y.M.Y.E.K.; methodology, A.M.E.-B. and A.F.H.; software, A.M.E.-B.; writing—original draft preparation, A.M.E.-B., A.M.I., W.F.S., T.A.S., A.O.A., M.I.A., M.N.S. and Z.I.; writing—review and editing, S.M.E.-G., A.M.I. and Z.I. All authors have read and agreed to the published version of the manuscript.

**Funding:** This work was supported by the Deanship of Scientific Research, Vice Presidency for Graduate Studies and Scientific Research, King Faisal University, Saudi Arabia, (GRANT773).

**Institutional Review Board Statement:** Not applicable.

**Informed Consent Statement:** Not applicable.

**Data Availability Statement:** Not applicable.

**Acknowledgments:** Authors extend their appreciation to the Deanship of Scientific Research, Vice Presidency for Graduate Studies and Scientific Research, King Faisal University, Saudi Arabia, for supporting this research work through grant number GRANT773.

**Conflicts of Interest:** The authors declare no conflict of interests.

## References

1. Faostat. Food and Agriculture Organization of the United Nations Statistics Division. Available online: <http://faostat3.fao.org/home/E> (accessed on 4 May 2022).
2. Cooke, W.B. Cephalosporium-artige schimmelpilze (hyphomycetes). *Mycologia* **1973**, *65*, 253–257. [[CrossRef](#)]
3. El-Shafey, H.; Abd-El-Rahim, M.; Refaat, M. A New Cephalosporium-Wilt Disease of Grain Sorghum in Egypt. In Proceedings of the Egyptian Phytopathology Congress, Cairo, Egypt, 26–29 November 1979; The Egyptian Phytopathology Society: Cairo, Egypt, 1980.
4. Rodrigues, R.T.; de Souza Silva, M.M.; de Oliveira, D.M.; Simplicio, J.B.; Costa, C.M.C.; de Siqueira, V.M. Endophytic fungi from *Sorghum bicolor* (L.) Moench: Influence of genotypes and crop systems and evaluation of antimicrobial activity. *J. Agric. Sci. Technol.* **2018**, *8*, 267–277.
5. Natural, M.; Frederiksen, R.; Rosenow, D. Acremonium wilt of sorghum [*Sorghum bicolor*, *Acremonium strictum*]. *Plant Dis.* **1982**, *66*, 863–865. [[CrossRef](#)]
6. Ali, M.; Osman, E.; Ibrahim, T.; Khalafalla, G.; Amin, G. In vitro antagonism between soil rhizosphere microorganisms and *acremonium strictum* the causal fungus of acremonium wilt in grain sorghum. *J. Agric. Sci. Mansoura Univ.* **2004**, *29*, 5821–5833. [[CrossRef](#)]
7. Salama, S. Investigations of the major stalk, foliar and grain disease of sorghum (*Sorghum bicolor*) including studies on the genetic nature of resistance. *Ann. Rep. Public Law* **1976**, *63*, 1–17.
8. Prasad, R.; Bhattacharyya, A.; Nguyen, Q.D. Nanotechnology in sustainable agriculture: Recent developments, challenges, and perspectives. *Front. Microbiol.* **2017**, *8*, 01014. [[CrossRef](#)] [[PubMed](#)]
9. El-Beltagi, H.S.; Ali, M.R.; Ramadan, K.M.A.; Anwar, R.; Shalaby, T.A.; Rezk, A.A.; El-Ganainy, S.M.; Mahmoud, S.F.; Alkafafy, M.; El-Mogy, M.M. Exogenous postharvest application of calcium chloride and salicylic acid to maintain the quality of broccoli florets. *Plants* **2022**, *11*, 1513. [[CrossRef](#)] [[PubMed](#)]
10. Parisi, C.; Vignani, M.; Rodríguez-Cerezo, E. Agricultural nanotechnologies: What are the current possibilities? *Nano Today* **2015**, *10*, 124–127. [[CrossRef](#)]
11. Khatoon, U.T.; Rao, G.N.; Mohan, K.M.; Ramanaviciene, A.; Ramanavicius, A. Antibacterial and antifungal activity of silver nanospheres synthesized by tri-sodium citrate assisted chemical approach. *Vacuum* **2017**, *146*, 259–265. [[CrossRef](#)]
12. Khatoon, U.T.; Rao, G.N.; Mohan, M.K.; Ramanaviciene, A.; Ramanavicius, A. Comparative study of antifungal activity of silver and gold nanoparticles synthesized by facile chemical approach. *J. Environ. Chem. Eng.* **2018**, *6*, 5837–5844. [[CrossRef](#)]
13. El-Gazzar, N.; Ismail, A.M. The potential use of titanium, silver and selenium nanoparticles in controlling leaf blight of tomato caused by *Alternaria alternata*. *Biocatal. Agric. Biotechnol.* **2020**, *27*, 101708. [[CrossRef](#)]
14. Ismail, A.M. Efficacy of copper oxide and magnesium oxide nanoparticles on controlling black scurf disease on potato. *Egypt. J. Phytopathol.* **2021**, *49*, 116–130. [[CrossRef](#)]
15. Ismail, A.M.; El-Gawad, A.; Mona, E. Antifungal activity of mgo and zno nanoparticles against powdery mildew of pepper under greenhouse conditions. *Egypt. J. Agric. Res.* **2021**, *99*, 421–434.
16. Raveendran, P.; Fu, J.; Wallen, S.L. Completely “green” synthesis and stabilization of metal nanoparticles. *J. Am. Chem. Soc.* **2003**, *125*, 13940–13941. [[CrossRef](#)] [[PubMed](#)]
17. Prasad, R.; Kumar, V.; Prasad, K.S. Nanotechnology in sustainable agriculture: Present concerns and future aspects. *Afr. J. Biotechnol.* **2014**, *13*, 705–713.
18. Prasad, R.; Gupta, N.; Kumar, M.; Kumar, V.; Wang, S.; Abd-El Salam, K.A. Nanomaterials act as plant defense mechanism. In *Nanotechnology*; Springer: Berlin/Heidelberg, Germany, 2017; pp. 253–269.
19. Mohapatra, M.; Anand, S. Synthesis and applications of nano-structured iron oxides/hydroxides—A review. *Int. J. Eng. Technol.* **2010**, *2*, 127–146. [[CrossRef](#)]
20. Fang, S.; Bresser, D.; Passerini, S. Transition metal oxide anodes for electrochemical energy storage in lithium- and sodium-ion batteries. *Adv. Energy Mater.* **2020**, *10*, 1902485. [[CrossRef](#)]
21. Tuharin, K.; Turek, Z.; Zanaška, M.; Kudrna, P.; Tichý, M. Iron oxide and iron sulfide films prepared for dye-sensitized solar cells. *Materials* **2020**, *13*, 1797. [[CrossRef](#)] [[PubMed](#)]

22. Wang, Q.; Ma, Y.; Liu, L.; Yao, S.; Wu, W.; Wang, Z.; Lv, P.; Zheng, J.; Yu, K.; Wei, W. Plasma enabled Fe<sub>2</sub>O<sub>3</sub>/Fe<sub>3</sub>O<sub>4</sub> nano-aggregates anchored on nitrogen-doped graphene as anode for sodium-ion batteries. *Nanomaterials* **2020**, *10*, 782. [[CrossRef](#)]
23. Cichello, S.A. Oxygen absorbers in food preservation: A review. *J. Food Sci. Technol.* **2015**, *52*, 1889–1895. [[CrossRef](#)] [[PubMed](#)]
24. Magro, M.; Baratella, D.; Bonaiuto, E.; de A. Roger, J.; Vianello, F. New perspectives on biomedical applications of iron oxide nanoparticles. *Curr. Med. Chem.* **2018**, *25*, 540–555. [[CrossRef](#)]
25. Rui, M.; Ma, C.; Hao, Y.; Guo, J.; Rui, Y.; Tang, X.; Zhao, Q.; Fan, X.; Zhang, Z.; Hou, T. Iron oxide nanoparticles as a potential iron fertilizer for peanut (*Arachis hypogaea*). *Front. Plant Sci.* **2016**, *7*, 815. [[CrossRef](#)] [[PubMed](#)]
26. Noqta, O.A.; Aziz, A.A.; Usman, I.A.; Bououdina, M. Recent advances in iron oxide nanoparticles (ionps): Synthesis and surface modification for biomedical applications. *J. Supercond. Nov. Magn. J.* **2019**, *32*, 779–795. [[CrossRef](#)]
27. Suturen, S.; Kaveev, A.; Korovin, A.; Fedorov, V.; Sawada, M.; Sokolov, N. Structural transformations and interfacial iron reduction in heterostructures with epitaxial layers of 3d metals and ferrimagnetic oxides. *J. Appl. Crystallogr.* **2018**, *51*, 1069–1081. [[CrossRef](#)]
28. Serga, V.; Burve, R.; Maiorov, M.; Krumina, A.; Skaudžius, R.; Zarkov, A.; Kareiva, A.; Popov, A.I. Impact of gadolinium on the structure and magnetic properties of nanocrystalline powders of iron oxides produced by the extraction-pyrolytic method. *Materials* **2020**, *13*, 4147. [[CrossRef](#)] [[PubMed](#)]
29. Xia, T.; Wang, J.; Wu, C.; Meng, F.; Shi, Z.; Lian, J.; Feng, J.; Meng, J. Novel complex-coprecipitation route to form high quality triethanolamine-coated Fe<sub>3</sub>O<sub>4</sub> nanocrystals: Their high saturation magnetizations and excellent water treatment properties. *CrystEngComm* **2012**, *14*, 5741–5744. [[CrossRef](#)]
30. Fahmy, H.M.; Moseleh, A.M.; Abd Elghany, A.; Shams-Eldin, E.; Serea, E.S.A.; Ali, S.A.; Shalan, A.E. Coated silver nanoparticles: Synthesis, cytotoxicity, and optical properties. *RSC Adv.* **2019**, *9*, 20118–20136. [[CrossRef](#)]
31. Arias, L.S.; Pessan, J.P.; Vieira, A.P.M.; Lima, T.M.T.d.; Delbem, A.C.B.; Monteiro, D.R. Iron oxide nanoparticles for biomedical applications: A perspective on synthesis, drugs, antimicrobial activity, and toxicity. *Antibiotics* **2018**, *7*, 46. [[CrossRef](#)] [[PubMed](#)]
32. Liu, J.-F.; Zhao, Z.-S.; Jiang, G.-B. Coating Fe<sub>3</sub>O<sub>4</sub> magnetic nanoparticles with humic acid for high efficient removal of heavy metals in water. *Environ. Sci. Technol.* **2008**, *42*, 6949–6954. [[CrossRef](#)] [[PubMed](#)]
33. Illés, E.; Tombácz, E. The effect of humic acid adsorption on pH-dependent surface charging and aggregation of magnetite nanoparticles. *J. Colloid Interface Sci.* **2006**, *295*, 115–123. [[CrossRef](#)] [[PubMed](#)]
34. Chekli, L.; Phuntsho, S.; Roy, M.; Shon, H.K. Characterisation of Fe-oxide nanoparticles coated with humic acid and suwannee river natural organic matter. *Sci. Total Environ.* **2013**, *461*, 19–27. [[CrossRef](#)] [[PubMed](#)]
35. Cuenya, B.R. Synthesis and catalytic properties of metal nanoparticles: Size, shape, support, composition, and oxidation state effects. *Thin Solid Films* **2010**, *518*, 3127–3150. [[CrossRef](#)]
36. Wu, S.; Sun, A.; Zhai, F.; Wang, J.; Xu, W.; Zhang, Q.; Volinsky, A.A. Fe<sub>3</sub>O<sub>4</sub> magnetic nanoparticles synthesis from tailings by ultrasonic chemical co-precipitation. *Mater. Lett.* **2011**, *65*, 1882–1884. [[CrossRef](#)]
37. Narayanan, K.B.; Sakthivel, N. Biological synthesis of metal nanoparticles by microbes. *Adv. Colloid. Interface Sci.* **2010**, *156*, 1–13. [[CrossRef](#)] [[PubMed](#)]
38. Ali, A.; Zafar, H.; Zia, M.; ul Haq, I.; Phull, A.R.; Ali, J.S.; Hussain, A. Synthesis, characterization, applications, and challenges of iron oxide nanoparticles. *Nanotechnol. Sci. Appl.* **2016**, *9*, 49–67. [[CrossRef](#)] [[PubMed](#)]
39. Koesnarpadi, S.; Santosa, S.J.; Siswanta, D.; Rusdiarso, B. Synthesis and characterization of magnetite nanoparticle coated humic acid (Fe<sub>3</sub>O<sub>4</sub>/ha). *Procedia Environ. Sci.* **2015**, *30*, 103–108. [[CrossRef](#)]
40. Gonçalves, L.; Seabra, A.B.; Pelegrino, M.T.; De Araujo, D.; Bernardes, J.S.; Haddad, P.S. Superparamagnetic iron oxide nanoparticles dispersed in pluronic f127 hydrogel: Potential uses in topical applications. *RSC Adv.* **2017**, *7*, 14496–14503. [[CrossRef](#)]
41. Enneffati, M.; Rasheed, M.; Louati, B.; Guidara, K.; Barillé, R. Morphology, uv-visible and ellipsometric studies of sodium lithium orthovanadate. *Opt. Quant. Electron.* **2019**, *51*, 1–19. [[CrossRef](#)]
42. Grover, R.; Moore, J. Toximetric studies of fungicides against brown rot organisms, *Sclerotinia fructicola* and *S. Laxa*. *Phytopathology* **1962**, *52*, 876–879.
43. Karunakar, R.; Pande, S.; Satyaprasad, K.; Ramarao, P. Varietal reaction of non-senescent sorghums to the pathogens causing root and stalk rot of sorghum in india. *Int. J. Pest Manag.* **1993**, *39*, 343–346. [[CrossRef](#)]
44. Azzam, C.R.; Atta, A.; Ismail, M. Development of molecular genetic markers for acremonium wilt disease resistance in grain sorghum. *Egypt. J. Plant Breed.* **2010**, *14*, 299–319.
45. Okamoto, M.; Hanada, A.; Kamiya, Y.; Yamaguchi, S.; Nambara, E. Measurement of abscisic acid and gibberellins by gas chromatography/mass spectrometry. In *Plant Hormones*; Springer: Berlin/Heidelberg, Germany, 2009; pp. 53–60.
46. Allam, A.; Hollis, J. Sulfide inhibition of oxidases in rice roots. *Phytopathology* **1972**, *62*, 634–639. [[CrossRef](#)]
47. Pereira, G.; Molina, S.; Lea, P.; Azevedo, R. Activity of antioxidant enzymes in response to cadmium in *Crotalaria juncea*. *Plant Soil* **2002**, *239*, 123–132. [[CrossRef](#)]
48. Mills, K.L.; Morton, R.; Page, G. *Textbook of Clinical Pathology*; Williams & Wilkins: Philadelphia, PA, USA, 1971.
49. Jain, N.C. *Schalm's Veterinary Hematology*; Lea and Febiger: Palo Alto, CA, USA, 1986.
50. Reitman, S.; Frankel, S. A colorimetric method for the determination of serum glutamic oxalacetic and glutamic pyruvic transaminases. *Am. J. Clin. Pathol.* **1957**, *28*, 56–63. [[CrossRef](#)] [[PubMed](#)]
51. Stevens, L.A.; Coresh, J.; Greene, T.; Levey, A.S. Assessing kidney function—Measured and estimated glomerular filtration rate. *N. Engl. J. Med.* **2006**, *354*, 2473–2483. [[CrossRef](#)] [[PubMed](#)]

52. Bancroft, J.D.; Gamble, M. *Theory and Practice of Histological Techniques*; Elsevier Health Sciences: Amsterdam, The Netherlands, 2008.
53. Snedecor, G.; Cochran, W. *Statistical Methods*, 7th ed.; Iowa State University Press: Ames, IA, USA, 1980.
54. Haydar, M.S.; Ghosh, S.; Mandal, P. Application of iron oxide nanoparticles as micronutrient fertilizer in mulberry propagation. *J. Plant Growth Regul.* **2021**, *41*, 1726–1746. [[CrossRef](#)]
55. Chandrasekar, N.; Kumar, K.; Balasubramnian, K.S.; Karunamurthy, K.; Varadharajan, R. Facile synthesis of iron oxide, iron-cobalt and zero valent iron nanoparticles and evaluation of their anti microbial activity, free radicle scavenging activity and antioxidant assay. *Dig. J. Nanomater. Bios.* **2013**, *8*, 765–775.
56. Parveen, S.; Wani, A.H.; Shah, M.A.; Devi, H.S.; Bhat, M.Y.; Koka, J.A. Preparation, characterization and antifungal activity of iron oxide nanoparticles. *Microb. Pathog.* **2018**, *115*, 287–292. [[CrossRef](#)]
57. Nehra, P.; Chauhan, R.; Garg, N.; Verma, K. Antibacterial and antifungal activity of chitosan coated iron oxide nanoparticles. *Br. J. Biomed. Sci.* **2018**, *75*, 13–18. [[CrossRef](#)]
58. Win, T.T.; Khan, S.; Bo, B.; Zada, S.; Fu, P. Green synthesis and characterization of Fe<sub>3</sub>O<sub>4</sub> nanoparticles using chlorella-k01 extract for potential enhancement of plant growth stimulating and antifungal activity. *Sci. Rep.* **2021**, *11*, 1–11. [[CrossRef](#)] [[PubMed](#)]
59. Hsueh, Y.-H.; Tsai, P.-H.; Lin, K.-S.; Ke, W.-J.; Chiang, C.-L. Antimicrobial effects of zero-valent iron nanoparticles on gram-positive bacillus strains and gram-negative *Escherichia coli* strains. *J. Nanobiotechnol.* **2017**, *15*, 1–12. [[CrossRef](#)]
60. Jindo, K.; Olivares, F.L.; Malcher, D.J.d.P.; Sánchez-Monedero, M.A.; Kempenaar, C.; Canellas, L.P. From lab to field: Role of humic substances under open-field and greenhouse conditions as biostimulant and biocontrol agent. *Front. Plant Sci.* **2020**, *11*, 426. [[CrossRef](#)] [[PubMed](#)]
61. Tomke, P.D.; Rathod, V.K. Facile fabrication of silver on magnetic nanocomposite (Fe<sub>3</sub>O<sub>4</sub>@ chitosan-agnp nanocomposite) for catalytic reduction of anthropogenic pollutant and agricultural pathogens. *Int. J. Biol. Macromol.* **2020**, *149*, 989–999. [[CrossRef](#)]
62. Ali, M.; Haroon, U.; Khizar, M.; Chaudhary, H.J.; Munis, M.F.H. Facile single step preparations of phyto-nanoparticles of iron in *Calotropis procera* leaf extract to evaluate their antifungal potential against *Alternaria alternata*. *Curr. Plant Biol.* **2020**, *23*, 100157. [[CrossRef](#)]
63. Devi, H.S.; Boda, M.A.; Shah, M.A.; Parveen, S.; Wani, A.H. Green synthesis of iron oxide nanoparticles using *Platanus orientalis* leaf extract for antifungal activity. *Green Process. Synth.* **2019**, *8*, 38–45. [[CrossRef](#)]
64. Crecchio, C.; Stotzky, G. Insecticidal activity and biodegradation of the toxin from *Bacillus thuringiensis* subsp. *Kurstaki* bound to humic acids from soil. *Soil Biol. Biochem.* **1998**, *30*, 463–470.
65. Wu, M.; Song, M.; Liu, M.; Jiang, C.; Li, Z. Fungicidal activities of soil humic/fulvic acids as related to their chemical structures in greenhouse vegetable fields with cultivation chronosequence. *Sci. Rep.* **2016**, *6*, 32858. [[CrossRef](#)] [[PubMed](#)]
66. Zhao, H.; Liu, Y.; Cui, Z.; Beattie, D.; Gu, Y.; Wang, Q. Design, synthesis, and biological activities of arylmethylamine substituted chlorotriazine and methylthiotriazine compounds. *J. Agric. Food Chem.* **2011**, *59*, 11711–11717. [[CrossRef](#)] [[PubMed](#)]
67. Abdeen, S.; Isaac, R.R.; Geo, S.; Sornalekshmi, S.; Rose, A.; Praseetha, P. Evaluation of antimicrobial activity of biosynthesized iron and silver nanoparticles using the fungi *Fusarium oxysporum* and *Actinomyces* sp. on human pathogens. *Nano Biomed. Eng.* **2013**, *5*, 39–45. [[CrossRef](#)]
68. Lee, C.; Kim, J.Y.; Lee, W.I.; Nelson, K.L.; Yoon, J.; Sedlak, D.L. Bactericidal effect of zero-valent iron nanoparticles on *Escherichia coli*. *Environ. Sci. Technol.* **2008**, *42*, 4927–4933. [[CrossRef](#)]
69. Behera, S.S.; Patra, J.K.; Pramanik, K.; Panda, N.; Thatoi, H. Characterization and evaluation of antibacterial activities of chemically synthesized iron oxide nanoparticles. *World J. Nano Sci. Eng.* **2012**, *2*, 196–200. [[CrossRef](#)]
70. Park, H.-J.; Kim, J.Y.; Kim, J.; Lee, J.-H.; Hahn, J.-S.; Gu, M.B.; Yoon, J. Silver-ion-mediated reactive oxygen species generation affecting bactericidal activity. *Water Res.* **2009**, *43*, 1027–1032. [[CrossRef](#)] [[PubMed](#)]
71. Keenan, C.R.; Sedlak, D.L. Factors affecting the yield of oxidants from the reaction of nanoparticulate zero-valent iron and oxygen. *Environ. Sci. Technol.* **2008**, *42*, 1262–1267. [[CrossRef](#)] [[PubMed](#)]
72. Zhang, W.; Dick, W.; Hoitink, H. Compost-induced systemic acquired resistance in cucumber to pythium root rot and anthracnose. *Phytopathology* **1996**, *86*, 1066–1070. [[CrossRef](#)]
73. Loffredo, E.; Berloco, M.; Casulli, F.; Senesi, N. In vitro assessment of the inhibition of humic substances on the growth of two strains of *Fusarium oxysporum*. *Biol. Fertil. Soils* **2007**, *43*, 759–769. [[CrossRef](#)]
74. Ali, M.; Osman, E.A.; Dawoud, E.I.; Ibrahim, T.F.; Amin, G. Optimization of the bioagent *Bacillus subtilis* biomass production and antibiosis against *Acremonium strictum*. *J. Soil Sci. Agric. Eng.* **2007**, *32*, 4075–4090. [[CrossRef](#)]
75. Yuan, J.; Chen, Y.; Li, H.; Lu, J.; Zhao, H.; Liu, M.; Nechitaylo, G.S.; Glushchenko, N.N. New insights into the cellular responses to iron nanoparticles in *Capsicum annuum*. *Sci. Rep.* **2018**, *8*, 3228. [[CrossRef](#)] [[PubMed](#)]
76. Elanchezian, R.; Kumar, D.; Ramesh, K.; Biswas, A.K.; Guhey, A.; Patra, A.K. Morpho-physiological and biochemical response of maize (*Zea mays* L.) plants fertilized with nano-iron (Fe<sub>3</sub>O<sub>4</sub>) micronutrient. *J. Plant Nutr.* **2017**, *40*, 1969–1977. [[CrossRef](#)]
77. Li, J.; Ma, Y.; Xie, Y. Stimulatory effect of Fe<sub>3</sub>O<sub>4</sub> nanoparticles on the growth and yield of *Pseudostellaria heterophylla* via improved photosynthetic performance. *HortScience* **2021**, *56*, 753–761. [[CrossRef](#)]
78. Bystrzejewska-Piotrowska, G.; Asztemborska, M.; Stęborowski, R.; Polkowska-Motrenko, H.; Danko, B.; Ryniewicz, J. Application of neutron activation for investigation of Fe<sub>3</sub>O<sub>4</sub> nanoparticles accumulation by plants. *Nukleonika* **2012**, *57*, 427–430.
79. Yigit, V.; Dikilitaş, M. Effect of humic acid applications on the root-rot diseases caused by *Fusarium* spp. on tomato plants. *Plant Pathol. J.* **2008**, *7*, 179–182. [[CrossRef](#)]

80. Abd-El-Kareem, F.; Abd-El-Latif, F.M.; Fotouh, Y. Integrated treatments between humic acid and sulfur for controlling early blight disease of potato plants under field infection. *Res. J. Agric. Biol. Sci.* **2009**, *5*, 1039–1045.
81. Ali, E.; Abd El-Rahman, K.; El-Far, I.; Mohamed, A. Response of some grain sorghum genotypes to foliar spray by humic acid. *Assiut J. Agric. Sci.* **2020**, *51*, 54–63.
82. Pirmohamed, T.; Dowding, J.M.; Singh, S.; Wasserman, B.; Heckert, E.; Karakoti, A.S.; King, J.E.; Seal, S.; Self, W.T. Nanoceria exhibit redox state-dependent catalase mimetic activity. *Chem. Commun.* **2010**, *46*, 2736–2738. [[CrossRef](#)] [[PubMed](#)]
83. Wei, H.; Wang, E. Nanomaterials with enzyme-like characteristics (nanozymes): Next-generation artificial enzymes. *Chem. Soc. Rev.* **2013**, *42*, 6060–6093. [[CrossRef](#)]
84. Penel, C.; Gaspar, T.; Greppin, H. *Plant Peroxidases, 1980–1990: Topics and Detailed Literature on Molecular, Biochemical, and Physiological Aspects*; University of Geneva: Geneva, Switzerland, 1992.
85. Ramanaviciene, A.; Acaite, J.; Ramanavicius, A.; Ramanavicius, A. Chronic caffeine intake affects lysozyme activity and immune cells in mice. *J. Pharm. Pharmacol.* **2004**, *56*, 671–676. [[CrossRef](#)]
86. Li, Y.; Wang, Z.; Liu, R. Superparamagnetic  $\alpha$ -Fe<sub>2</sub>O<sub>3</sub>/Fe<sub>3</sub>O<sub>4</sub> heterogeneous nanoparticles with enhanced biocompatibility. *Nanomaterials* **2021**, *11*, 834. [[CrossRef](#)]
87. Ramanaviciene, A.; Kausaite, A.; Tautkus, S.; Ramanavicius, A. Biocompatibility of polypyrrole particles: An in-vivo study in mice. *J. Pharm. Pharmacol.* **2007**, *59*, 311–315. [[CrossRef](#)] [[PubMed](#)]
88. Parivar, K.; Malekvand Fard, F.; Bayat, M.; Alavian, S.M.; Motavaf, M. Evaluation of iron oxide nanoparticles toxicity on liver cells of balb/c rats. *Iran. Red Crescent Med. J.* **2016**, *18*, e28939. [[CrossRef](#)]
89. Kim, J.S.; Yoon, T.-J.; Yu, K.N.; Kim, B.G.; Park, S.J.; Kim, H.W.; Lee, K.H.; Park, S.B.; Lee, J.-K.; Cho, M.H. Toxicity and tissue distribution of magnetic nanoparticles in mice. *Toxicol. Sci.* **2006**, *89*, 338–347. [[CrossRef](#)]
90. Salehi, M.; Fatahian, S.; Shahanipour, K. Effect of iron oxide nanoparticles coated with chitosan on renal functional indices in rats. *J. Gorgan. Univ. Med. Sci.* **2017**, *19*, 14–19.
91. Battis, G.N., Jr. The enigma of liver enzymes: Transferases. *J. Insur. Med.* **1988**, *20*, 17–20.
92. Vozarova, B.; Stefan, N.; Lindsay, R.S.; Saremi, A.; Pratley, R.E.; Bogardus, C.; Tataranni, P.A. High alanine aminotransferase is associated with decreased hepatic insulin sensitivity and predicts the development of type 2 diabetes. *Diabetes* **2002**, *51*, 1889–1895. [[CrossRef](#)] [[PubMed](#)]
93. Sadeghi, L.; Tanwir, F.; Babadi, V.Y. In vitro toxicity of iron oxide nanoparticle: Oxidative damages on hep g2 cells. *Exp. Toxicol. Pathol.* **2015**, *67*, 197–203. [[CrossRef](#)] [[PubMed](#)]